

Seismic Energy Transmission in an Intensively Scattering Environment*

Yosio Nakamura

Geophysics Laboratory, Marine Science Institute, University of Texas,
700 The Strand, Galveston, Texas 77550, USA

Abstract. For describing transmission of seismic energy through a medium in which seismic waves are intensively scattered, a statistical approach provides an attractive alternative to the conventional, deterministic approach. The energy transmission in such a medium with a given size distribution of scatterers is generally governed by a diffusion equation with a frequency-dependent diffusivity, rather than wave equations as in the conventional approach. By applying this theory, we can explain many unusual characteristics of lunar seismic signals, including those generated by surface impacts at near and far ranges and by continuous movement of the Lunar Rovers. The size distribution of scatterers can be estimated from the frequency dependence of diffusivity. Predominantly rectilinear particle motions observed indicate that the scattered energy is transmitted as body waves. When intensive scattering is limited to only a part of the transmitting medium, as in the case of far impacts on the moon, a more general theory combining the two approaches is required. The theory is also useful for interpreting certain characteristics of terrestrial seismic signals because, while frequently ignored, appreciable scattering exists even for terrestrial cases.

Key words: Seismic scattering — Lunar seismic signals.

1. Introduction

Scattering of seismic waves in a medium of randomly distributed heterogeneity may be described using the conventional seismic wave theory. When the scattering is intense, however, this deterministic approach becomes increasingly difficult, and some alternative may be more convenient. In this paper, therefore, I will present such an alternative approach, namely, the seismic diffusion theory.

The data taken by the Apollo lunar seismometers compelled one to look for such alternatives. An example of a lunar seismogram is shown in Figure 1. The

* Marine Science Institute, Geophysics Laboratory, Contribution No. 195

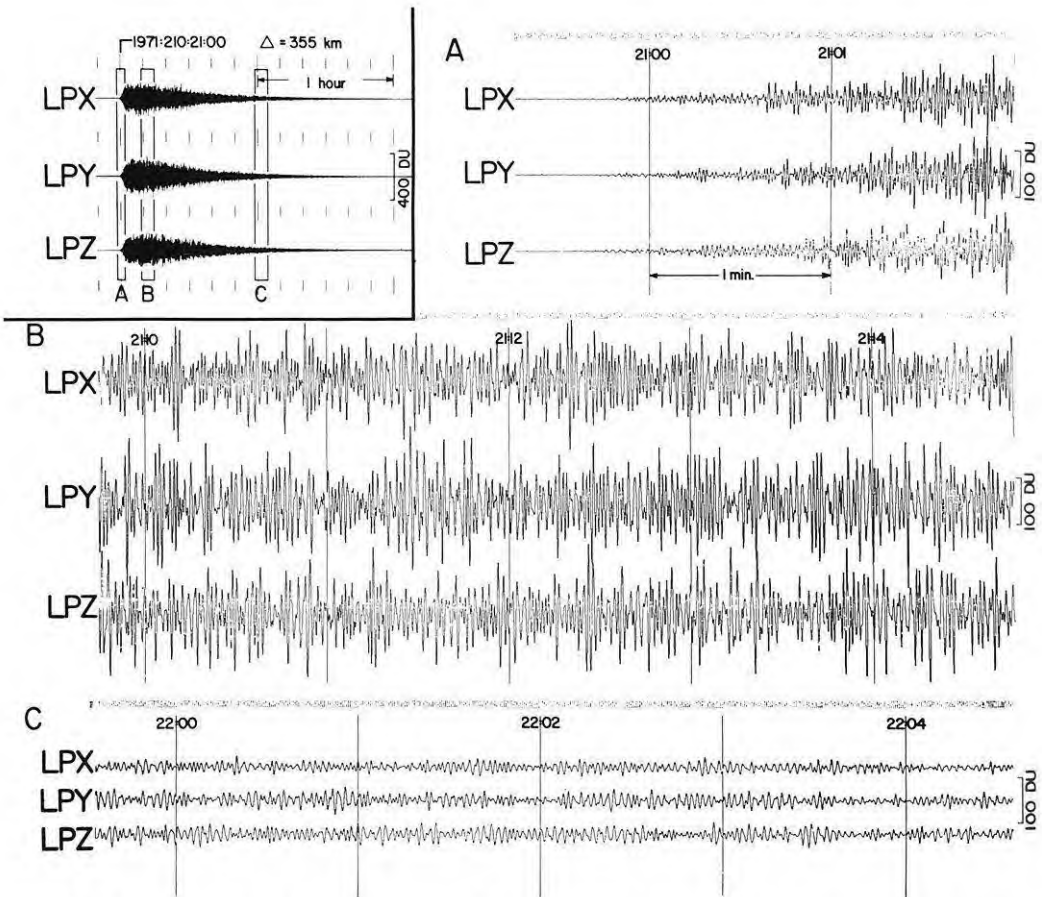


Fig. 1. An example of lunar seismograms, showing the entire wave train in a compressed time scale (upper left) and selected portions in an expanded time scale. *LPX*, *LPY* and *LPZ* designate two horizontal and a vertical component, respectively, of the long-period instrument. *DU* stands for digital unit, the smallest digitization step, and corresponds to the ground displacement of about 80 μm at the peak of the instrument response (0.45 Hz). The seismogram shown is for the Apollo 15 S-IVB impact observed at the Apollo 12 station

most striking features of the seismogram are (1) the gradual build-up of the signal at the beginning, (2) extremely prolonged coda, and (3) lack of apparent coherence among 3 orthogonal components of ground motion. It is believed that these unusual characteristics of lunar seismograms are caused primarily by (1) intensive scattering of seismic waves, (2) trapping of seismic energy in the surface zone of the moon by a strong velocity gradient, and (3) very low attenuation of waves in the surface zone. Synthesizing a seismogram such as this through the conventional wave-theoretical approach seems hopeless; thus, there exists a strong need for alternative approaches.

In this paper, first I will briefly review the development of the seismic diffusion theory for a medium with randomly distributed scatterers of a given size distribu-

tion; then give some examples of how this theory is applied to real situations; and finally, discuss some further properties of scattered seismic signals and outstanding problems.

A precautionary statement before we continue: In adopting this new approach, we are not denying the wave nature of seismic waves. We are simply looking at the same phenomenon from a different point of view. The approach we are taking is statistical in contrast to the deterministic approach for the conventional wave theory. The two approaches might be considered to be similar to the wave/particle duality of electromagnetic radiation.

2. Seismic Diffusion Theory

2.1. Diffusion in a Distributed Scatterer Field

Let us consider a space filled with a large number of scatterers of various sizes. The situation is similar to scattering of ultrasonic waves by grains in polycrystalline materials, where it is generally found that (1) at low frequencies where wavelength, λ , is long compared with the average grain size, D , the phenomenon is essentially Rayleigh scattering, and the square root of the scattered power is proportional to $D^3 f^4$, where f is the frequency; (2) at intermediate frequencies where the wavelength is of the same order as the average grain size, the scattering is proportional to Df^2 ; and (3) at high frequencies where the wavelength is much shorter than the average grain size, the scattering is due purely to reflections and refractions, and is proportional to D^{-1} (Papadakis, 1968). This frequency dependence of intensity of scattering is schematically shown in Figure 2. Most theoretical works on scattering to date have been limited to the low-frequency region (1) for weak scattering. In reality, however, many seismic scattering problems cover the whole range of the D/λ relationship. For these cases, the detailed behavior of the transition

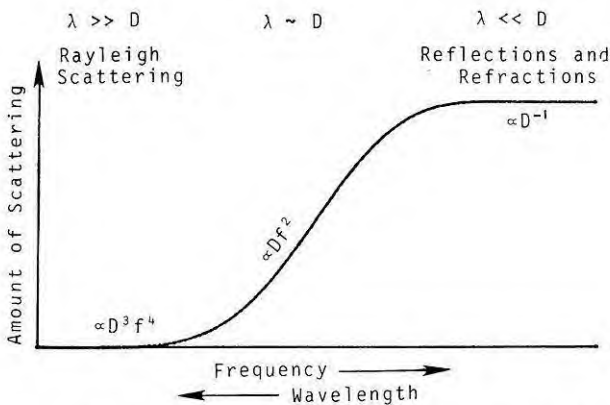


Fig. 2. Schematic diagram of the intensity of scattering as a function of the wavelength/scatter-size ratio. Though the diagram is drawn to show only the effect of varying f (or λ) for a fixed D , it may be interpreted to represent the effect of varying D for a fixed f or, more generally, the effect of varying both f and D .

from the low-frequency region to the high-frequency region of the scattering response becomes of less importance, and the curve of Figure 2 may be approximated by a step function; i.e., significant scattering occurs only when the scatterer size is greater than or equal to a certain fraction, k , of the wavelength:

$$D \geq k\lambda \quad (1)$$

With this approximation, we may treat seismic waves of a given wavelength as particles traveling through a space filled with scatterers, with more effective scatterers for shorter wavelength because we count only those scatterers that satisfy Equation (1).

Now let us further define the cumulative size distribution of hypothetical, circular (in a two-dimensional space) or spherical (in a three-dimensional space), non-overlapping scatterers to be given by a linear relation in log-log scales:

$$\log N = a - b \log D, \quad D \leq D_m \quad (2)$$

where N is the number per unit space of scatterers of diameter greater than or equal to D , a and b are constants, and D_m is the diameter of the largest scatterer in the field.

Retaining the particle-like treatment of seismic waves, the probability that a seismic wave of wavelength λ is scattered within a distance of travel x can be obtained as the probability of encounter of the wave with any of the scatterers that satisfy the relation (1) and distributed according to the relation (2), and is given by (Nakamura, 1976):

$$P(x) = 1 - \exp\{-xf(\lambda)\} \quad (3)$$

where

$$\begin{aligned} f(\lambda) &= 10^a b(1-b)^{-1} \{D_m^{1-b} - (k\lambda)^{1-b}\}, \quad b \neq 1 \\ &= 10^a \log(D_m/k\lambda), \quad b = 1 \end{aligned} \quad (4)$$

The mean free path, μ , of the seismic wave in such a field, therefore is given by

$$\mu = \int_0^{\infty} \{1 - P(x)\} dx = f(\lambda)^{-1} \quad (5)$$

When the fractional changes in the seismic energy density, E , and the seismic energy flow, J , per mean free path are small, an approximate relation

$$J = -(v\mu/n) \text{grad } E \quad (6)$$

holds for an n -dimensional space, where v is the seismic wave velocity (cf. Morse and Feshback, 1953, p. 178). On the other hand, the requirement for the conservation of energy leads to the equation of continuity

$$\partial E/\partial t = -\text{div } J - \omega E/Q \quad (7)$$

where t is the time, ω is the angular frequency and Q^{-1} is the dissipation function for the seismic energy. We thus obtain from Equations (6) and (7),

$$\partial E/\partial t = (v\mu/n) \nabla^2 E - \omega E/Q \quad (8)$$

This, except for the dissipation term, is the diffusion equation with a diffusivity $d = v\mu/n$, which is frequency dependent through Equations (4) and (5).

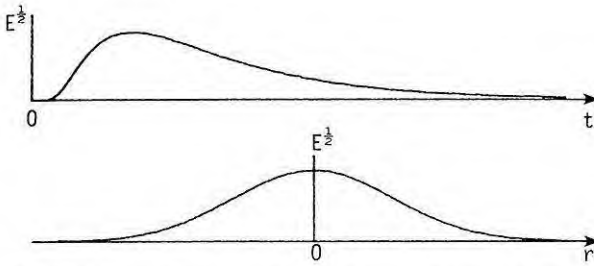


Fig. 3. Schematic diagrams showing the general shapes of the square root of the energy density resulting from an impulsive point source. The upper diagram shows the variation with time at a given distance, and should approximate the observed signal envelope. The lower diagram shows the variation with distance at a given time, and displays the concentration of energy near the source

2.2. Impulsive Point Source

A solution of Equation (8) that satisfies the conditions for an impulsive energy source at a point in a two-dimensional space is

$$E = E_0 (\pi \xi t)^{-1} \exp(-r^2/\xi t - \omega t/Q) \quad (9)$$

while for a three dimensional space, it is

$$E = E_0 (\pi \xi t)^{-3/2} \exp(-r^2/\xi t - \omega t/Q) \quad (10)$$

where E_0 is the seismic energy released at the point source, r is the radial distance from the source, and

$$\xi = 4d = 4v\mu/n. \quad (11)$$

At a given distance, the square root of the energy density, Equation (9) or (10), varies with time as depicted in the upper diagram of Figure 3. Good agreement of this shape with that of the envelope of the lunar impact seismogram in Figure 1 suggests that the intensive scattering in the moon is indeed responsible for the unusual characteristics of the lunar seismic signals.

The lower diagram of Figure 3 shows how the square root of energy density varies with respect to the distance from the source at a given time. It is seen that the largest amount of energy is always found near the source. In the near-source region, the scattered energy density is nearly independent of distance. This is in agreement with the observations by Aki and Chouet (1975) of the coda waves from local earthquakes, which are interpreted as scattered waves.

3. Applications

3.1. Lunar Impact Signals

The unusual characteristics of lunar seismic signals as described earlier can readily be explained by the diffusion approach (Latham et al., 1970; Dainty et al.,

1974). The observed envelopes agree well with theoretical expectations except for the first few seconds, when non-scattered, radially transmitting waves are still dominant. For the major part of the signal, one can determine the apparent diffusivity and the dissipation factor by fitting a set of theoretical curves with observed signal envelopes; "apparent" because the theory, as described in the preceding section, assumes a constant diffusivity, while in the real moon it is more likely to be depth-dependent as will be discussed later. The apparent diffusivity thus determined is strongly frequency dependent, decreasing rapidly with increasing frequency, as expected from the theory. On the other hand, the dissipation factor is nearly independent of frequency for most impact signals, giving a Q of the order of 6000.

3.2. Signals from Lunar Rovers

Seismic signals generated by the movement of the lunar roving vehicles (Rovers: vehicles used for lunar surface transportation during the Apollo 15 and 16 missions) possessed some unusual properties. The variation of the observed signal amplitude was relatively smooth despite the irregular movement of the Rovers. The starting and stopping of a Rover produced only very gradual build-up and decay of observed signal intensity, taking several minutes, rather than abrupt changes. The observed amplitude at a given distance was smaller, by a factor of up to three, when a Rover was coming back towards the seismic station than when it was moving away from the station. These unusual characteristics can also be explained readily by the seismic diffusion theory (Nakamura, 1976).

A moving source such as a Rover may be considered as a succession of infinitesimal, impulsive, point sources, each of which has a seismic effect at the station represented by a formula of the type (9) or (10). We will here consider a two-dimensional case, represented by Equation (9), because the extremely high velocity gradient in the near-surface zone of the moon efficiently traps most of the seismic energy in a shallow zone, and the energy transmission, therefore, is essentially two dimensional for the short distances being considered. Thus, integrating Equation (9) rewritten for infinitesimal sources with respect to time, we obtain

$$E(r) = \int_{r_0/c}^{r/c} \frac{\varepsilon}{\pi \xi(t-\tau)} \exp \left\{ -\frac{(c\tau)^2}{\xi(t-\tau)} - \frac{\omega(t-\tau)}{Q} \right\} d\tau \quad (12)$$

for the energy density at the coordinate origin due to a moving source which has started from distance r_0 and is moving at a radial velocity of c at a distance of r .

The variation of seismic signal intensity obtained by evaluating Equation (12) indeed shows all the characteristics of the Rover signals described above. The diffusivity, ξ , is determined as a function of frequency, decreasing from about $0.03 \text{ km}^2/\text{s}$ at 4 Hz to about $0.02 \text{ km}^2/\text{s}$ at 8 Hz. The mean free path of seismic waves can be estimated from the observed diffusivity if a value for the seismic velocity, v , is assumed in Equation (11). Here, we must consider some sort of statistical average of velocities appropriate for the distance ranges being considered. If we use a velocity of 100 m/s, which is within a factor of 3 of velocities of

various possible modes of propagation in the lunar surface zone, the mean free path is estimated to be of the order of 100 m.

The theory as developed in the preceding section allows the size distribution of the scatterers to be determined from the observed frequency dependence of diffusivity, by working backward through Equations (11), (5), (4), and (2). The scatterer size distribution thus determined is found to be very close to the steady-state size distribution of craters on the lunar surface as corrected for overlapping craters. Thus, it is possible that the topographic and structural disturbances caused by cratering is responsible for the observed scattering of seismic waves.

3.3. Terrestrial Applications

The diffusion approach to the seismic scattering problem is not limited to the lunar applications. Terrestrial seismic signals in the near-source regions can often be interpreted in terms of diffusion-type scattering. Wesley (1965) interpreted seismic signals generated by an underground nuclear explosion in terms of diffusion. Aki (1969) and Aki and Chouet (1975) described the coda of small, local earthquakes in terms of scattered seismic waves nearly trapped in the source region, a phenomenon essentially equivalent to diffusion. Herrmann (1976, presented at this Symposium) attempted to synthesize the seismic coda of local earthquakes in terms of random-phased waves modulated by an empirically determined envelope function.

Wesley's values of diffusivity found for the terrestrial case were of the same order as those for lunar impact signals at comparable distances. The apparent difference in wave characteristics between the terrestrial and lunar seismograms, therefore, seems to be primarily a difference in the dissipation characteristics of the transmitting media rather than a difference in degree of scattering.

4. Further Properties of Scattered Seismic Waves and Problems

4.1. Coherence and Phase Spectra

I have stated earlier that lunar seismograms show no "apparent" coherence among three orthogonal components of ground motion. However, this does not mean that the ground motion is completely random and that there is no coherent phase relation at all frequencies. Figures 4 and 5 show an example of coherence and phase spectra of lunar impact seismograms, calculated following Kanasevich (1973, pp. 115-116):

Coherence between x and y

$$= \frac{(\text{cospectrum of } x, y)^2 + (\text{quadrature spectrum of } x, y)^2}{(\text{power spectrum of } x) \cdot (\text{power spectrum of } y)} \quad (13)$$

and

Phase spectrum between x and y

$$= \tan^{-1} \left(\frac{\text{quadrature spectrum of } x, y}{\text{cospectrum of } x, y} \right). \quad (14)$$

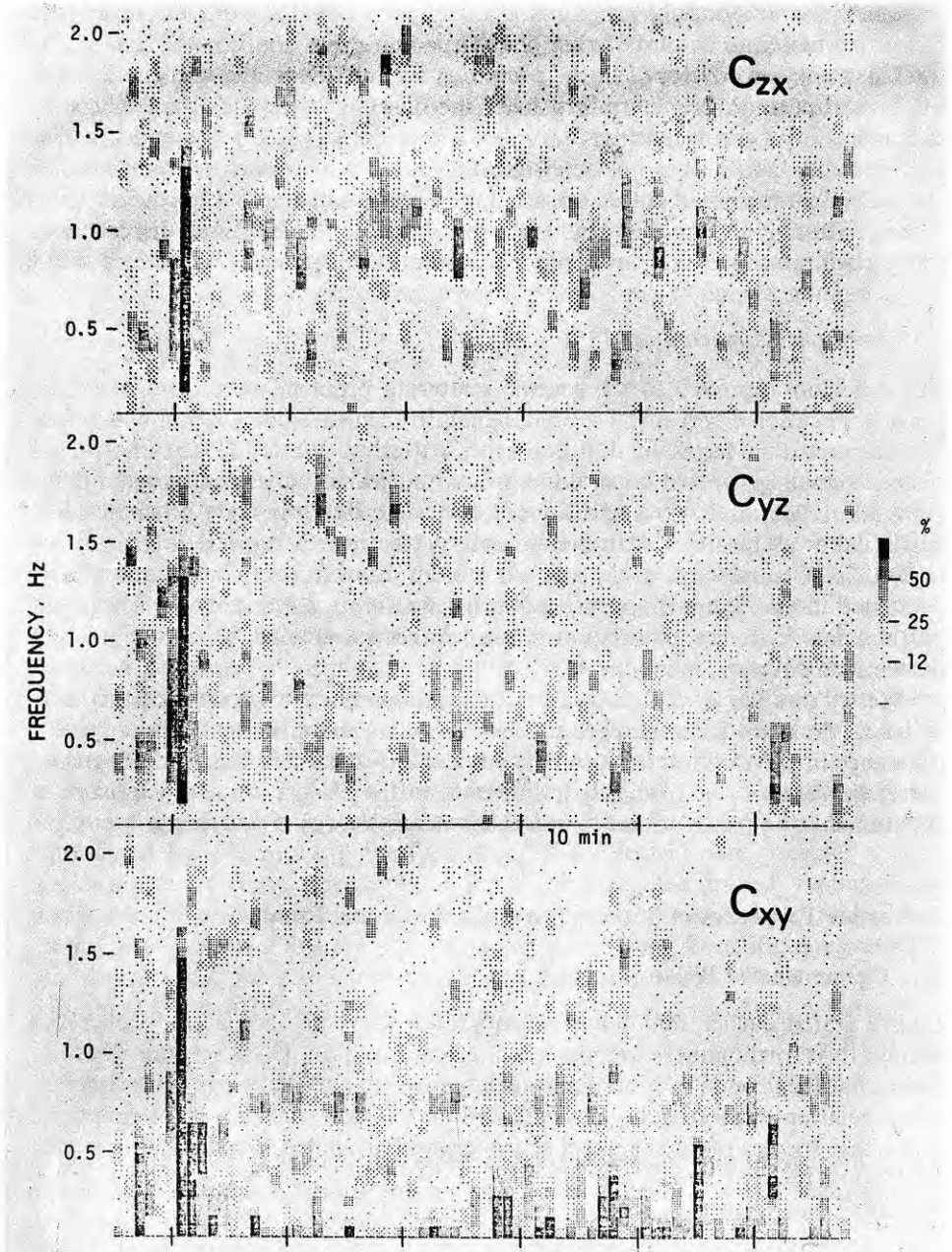


Fig. 4. A coherence spectrogram of a lunar impact signal. The degree of coherence is represented by the variation of density. C_{ij} represents the coherence between i and j components of ground motion. The signal begins about 5 min from the left edge of the diagram. The example shown is for the Apollo 14 LM impact observed at the Apollo 14 station

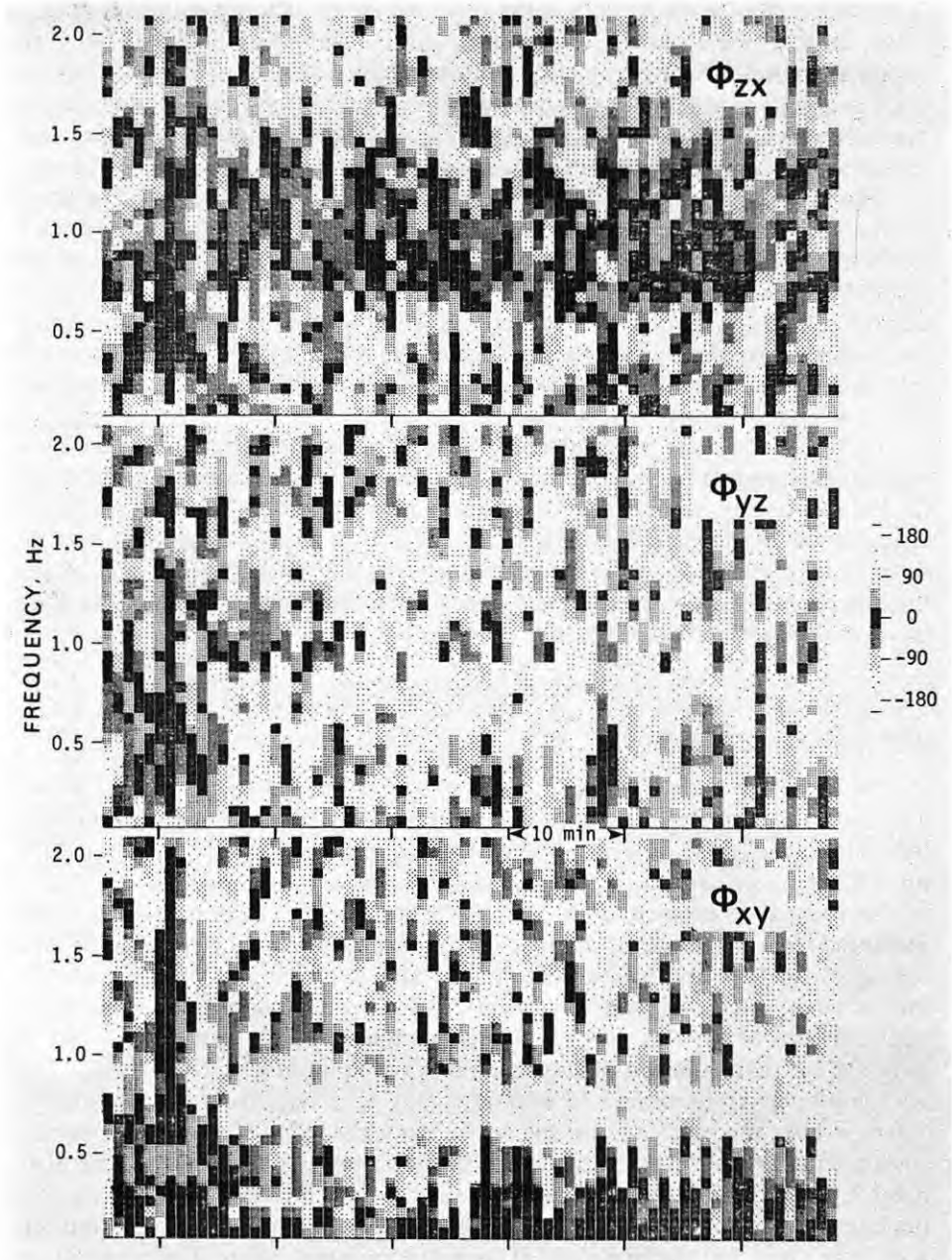


Fig. 5. A phase spectrogram of a lunar impact signal. The phase relation is converted to the variation of density as indicated by the scale on the right. ϕ_{ij} represents the phase between i and j components of ground motion. The example shown is for the same seismogram as that of Figure 4, and covers the same time interval

The coherence is generally high at the very beginning of the signal, corresponding to the initial *P*-wave arrival. It is relatively low for the rest of the signal, but is not as low as expected for a completely random signal.

The observed coherence exceeds the square root of the variance of coherence for a completely random signal (about 6% for this example) more often than expected, particularly at certain frequencies.

The non-randomness of the lunar seismograms is more clearly demonstrated in the phase spectra, Figure 5. The phase relationship among components is predominantly in phase or 180° out of phase, indicating that the particle motion is predominantly rectilinear rather than elliptical, which would show 90° phase relations. The coherent phase relationship is particularly pronounced at certain frequency bands. At a given seismic station, the phase spectra of various seismic events exhibit essentially the same phase relations among components regardless of the azimuthal direction of the source.

These observations imply the following: (1) The predominantly rectilinear polarization suggests that the most scattered energy is in the form of body waves. (2) Polarization of seismic signals which is independent of the source azimuth suggests one or more predominant scatterers that happen to be located near the seismometer. The scatterers in the near-range thus determine the polarization and the coherence of the observed seismic signal, while those in the far range determine the overall envelope of the signal.

4.2. Long-Range Transmission

The scattering described in the preceding sections assumes a constant diffusivity throughout the medium. For many real cases, however, this simplistic model is not sufficient, and further refinements of the theory are required.

An immediate problem is the vertical heterogeneity. The apparent diffusivity measured from the envelope of lunar impact signals increases with distance, with the signal rise time approaching a constant value at far ranges. This suggests that the diffusivity increases with increasing depth, approaching infinity at a certain depth. At this depth, therefore, the diffusion equation no longer applies, and we must use the more conventional method of wave equations.

Long-range transmission of seismic energy thus requires a combination of diffusion near the surface zone and wave propagation at depths. For a surface source, such as a meteoroid impact on the moon, seismic waves are (1) first scattered in the surface zone, (2) leak gradually into the interior, (3) travel through the interior as ordinary seismic waves, (4) are absorbed in the surface scattering zone near the seismic station, and (5) are scattered again before final observation. The observed seismic wave train at far distances has a characteristic envelope consisting of two clearly identifiable scattered envelopes, one for *P*-waves and the other for *S*-waves, as seen for example in Figure 4 of Nakamura et al. (1976). This is because step (3) above separates these two wave trains. Theoretical formulations of steps (2) and (4) have not yet been worked out, and require further study.

5. Conclusions

The diffusion approach offers a very attractive alternative to the more conventional wave propagation approach for describing intensive scattering of seismic waves. Even a simple, constant-diffusivity model can explain many of the properties of scattered seismic wave trains. For applications to far ranges, a more sophisticated formulation combining the effects of diffusion and wave propagation is needed.

Acknowledgements. I wish to thank other team members of the Apollo Passive Seismic Experiment for stimulating discussions on this subject, and especially Dr. G. V. Latham and Dr. H. J. Dorman for critically reviewing the manuscript. This research was supported by NASA under Contract NAS 9-14581.

References

- Aki, K.: Analysis of the seismic coda of local earthquakes as scattered waves. *J. Geophys. Res.* **74**, 615–631, 1969
- Aki, K., Chouet, B.: Origin of coda waves: source, attenuation, and scattering effects. *J. Geophys. Res.* **80**, 3322–3342, 1975
- Dainty, A. M., Toksöz, M. N., Anderson, K. R., Pines, P. J., Nakamura, Y., Latham, G.: Seismic scattering and shallow structure of the moon in Oceanus Procellarum. *The Moon* **9**, 11–29, 1974
- Kanasewich, E. R.: Time sequence analysis in geophysics. Edmonton: University of Alberta Press 1973
- Latham, G. V., Ewing, M., Press, F., Sutton, G., Dorman, J., Nakamura, Y., Toksöz, N., Wiggins, R., Derr, J., Duennebier, F.: Passive seismic experiment. *Science* **167**, 455–457, 1970
- Morse, P. M., Feshback, H.: *Method of theoretical physics, Pt. I.* New York: McGraw-Hill 1953
- Nakamura, Y.: Seismic energy transmission in the lunar surface zone determined from signals generated by movement of lunar rovers. *Bull. Seism. Soc. Am.* **66**, 593–606, 1976
- Nakamura, Y., Duennebier, F. K., Latham, G. V., Dorman, H. J.: Structure of the lunar mantle. *J. Geophys. Res.* **81**, 4818–4824, 1976
- Papadakis, E. P.: Ultrasonic attenuation caused by scattering in polycrystalline media. In: *Physical acoustics, Vol. IV, Pt. B*, W. P. Mason, ed., pp. 269–328. New York: Academic Press 1968
- Wesley, J. P.: Diffusion of seismic energy in the near range. *J. Geophys. Res.* **70**, 5099–5106, 1965

Received October 20, 1976; Revised Version December 21, 1976